

## Surfactant-free purification of membrane protein complexes from bacteria: application to the staphylococcal penicillin-binding protein complex PBP2/PBP2a

This content has been downloaded from IOPscience. Please scroll down to see the full text.

2014 Nanotechnology 25 285101

(<http://iopscience.iop.org/0957-4484/25/28/285101>)

View [the table of contents for this issue](#), or go to the [journal homepage](#) for more

### Download details:

IP Address: 193.61.255.84

This content was downloaded on 14/01/2016 at 15:46

Please note that [terms and conditions apply](#).

# Surfactant-free purification of membrane protein complexes from bacteria: application to the staphylococcal penicillin-binding protein complex PBP2/PBP2a

Sarah Paulin<sup>1</sup>, Mohammed Jamshad<sup>2</sup>, Timothy R Dafforn<sup>2</sup>,  
Jorge Garcia-Lara<sup>3</sup>, Simon J Foster<sup>3</sup>, Nicola F Galley<sup>4</sup>, David I Roper<sup>4</sup>,  
Helena Rosado<sup>1</sup> and Peter W Taylor<sup>1</sup>

<sup>1</sup> School of Pharmacy, University College London, 29-39 Brunswick Square, London WC1N 1AX, UK

<sup>2</sup> School of Biosciences, University of Birmingham, Edgbaston, Birmingham B15 2TT, UK

<sup>3</sup> Krebs Institute, University of Sheffield, Firth Court, Western Bank, Sheffield S10 2TN, UK

<sup>4</sup> School of Life Sciences, University of Warwick, Gibbet Hill Campus, Coventry CV4 7AL, UK

E-mail: [peter.taylor@ucl.ac.uk](mailto:peter.taylor@ucl.ac.uk)


Received 16 December 2013, revised 4 April 2014

Accepted for publication 22 April 2014

Published 27 June 2014

## Abstract

Surfactant-mediated removal of proteins from biomembranes invariably results in partial or complete loss of function and disassembly of multi-protein complexes. We determined the capacity of styrene-co-maleic acid (SMA) co-polymer to remove components of the cell division machinery from the membrane of drug-resistant staphylococcal cells. SMA-lipid nanoparticles solubilized FtsZ-PBP2-PBP2a complexes from intact cells, demonstrating the close physical proximity of these proteins within the lipid bilayer. Exposure of bacteria to (-)-epicatechin gallate, a polyphenolic agent that abolishes  $\beta$ -lactam resistance in staphylococci, disrupted the association between PBP2 and PBP2a. Thus, SMA purification provides a means to remove native integral membrane protein assemblages with minimal physical disruption and shows promise as a tool for the interrogation of molecular aspects of bacterial membrane protein structure and function.

 Online supplementary data available from [stacks.iop.org/NANO/25/285101/mmedia](http://stacks.iop.org/NANO/25/285101/mmedia)

Keywords: *Staphylococcus aureus*, poly(styrene-co-maleic acid), lipid nanoparticles, antibiotic resistance, immunoaffinity chromatography

(Some figures may appear in colour only in the online journal)

## 1. Introduction

Integral membrane proteins participate in a variety of activities essential for survival, homeostasis and division. Many function only within dynamic multi-protein assemblages embedded in specialized lipid microdomains of the bacterial

cytoplasmic membrane (CM). Thus, the bacterial cell division machinery is localized at mid-cell within a divisome of more than 20 proteins [1]; their dynamic and amphipathic nature makes them difficult to study in their native state, as their removal by surfactants leads to decreased structural integrity, complex disassembly and loss of activity. Advances in membrane solubilization have enabled surfactant-free extraction and purification of functionally active membrane proteins [2, 3]. Amphipathic poly(styrene-co-maleic acid) (SMA), soluble at neutral and alkaline pH and insoluble at



Content from this work may be used under the terms of the [Creative Commons Attribution 3.0 licence](http://creativecommons.org/licenses/by/3.0/). Any further distribution of this work must maintain attribution to the author(s) and the title of the work, journal citation and DOI.

lower pH, auto-assembles at neutral or alkaline pH into membranes to form discoidal nanostructures around membrane proteins and associated lipids. Preservation of the native lipid environment of embedded proteins yields correctly folded, functionally active protein. The technique has been used to remove and purify functionally active proteins from liposomes [2–4] and over-expressed proteins from isolated membranes of eukaryotes and prokaryotes. SMA-lipid particles (SMALPs) have also been employed to remove respiratory enzyme complexes from mitochondrial membranes [5], suggesting that SMALP encapsulation provides a tool to identify and characterize protein complexes in which monomeric components are in close physical proximity.

*Staphylococcus aureus* rapidly acquires genes encoding antibiotic resistance; strains resistant to  $\beta$ -lactam agents, typified by methicillin-resistant *S. aureus* (MRSA), are usually insensitive to other antibiotic classes and there are few treatment options [6]. MRSA is resistant to  $\beta$ -lactam drugs due to acquisition of the *mecA* gene encoding penicillin-binding protein (PBP) 2a, an enzyme that takes over the transpeptidase function of PBP2 following  $\beta$ -lactam inactivation of the PBP2 transpeptidase, to ensure continued synthesis of cell wall peptidoglycan [7]. PBPs are embedded in the CM, which is comprised of an asymmetric array of lipids with differing charge characteristics, in the main phosphatidylglycerol (PG), lysyl-PG and cardiolipin [8]. It has proven difficult to determine the spatial proximity of PBP2 and PBP2a in the CM, even though they form part of the cell division machinery at the division septum; divisome assembly is regulated by polymerization of the tubulin homologue FtsZ to a ring-like structure that acts as a scaffold for recruitment of other proteins, including PBPs [1, 9]. Membrane-intercalating agents that abrogate  $\beta$ -lactam resistance disperse PBP2 from the septum [8] and conversion to drug susceptibility may be due to disruption of functional and spatial associations between these proteins. We used the SMALP technique to determine that PBP2/PBP2a complexes can be captured together in nanoparticles from normally dividing MRSA cells and to demonstrate that the drug resistance modifier (-)-epicatechin gallate (ECg) alters the spatial relationship between the two proteins.

## 2. Experimental details

Epidemic MRSA isolate EMRSA-16 was from a clinical sample obtained at the Royal Free Hospital (London, UK). Methicillin-susceptible *S. aureus* SH1000 was obtained from Alex O'Neill (University of Leeds, UK). Bacteria were grown in Mueller-Hinton broth (Oxoid) to mid-logarithmic phase at 35 °C with constant agitation and aeration; PBP2a was induced with sub-inhibitory concentrations ( $125 \mu\text{g l}^{-1}$ ) of oxacillin. Lysostaphin, a glycine-glycine endopeptidase, and the protease and phosphatase inhibitor mixture HALT were purchased from Sigma-Aldrich. Anti-PBP2 antiserum was produced in rabbits with recombinant his<sub>6</sub>-tagged PBP2; mouse anti-PBP2a antibody was purchased from My Biosource and 1,2-dimyristoyl-sn-glycero-3-phosphocholine

(DMPC) from Avanti Polar Lipids. Rabbit anti-FtsZ antiserum was a gift from Jeff Errington (Newcastle University, UK). SMA was composed of styrene and maleic acid residues in a ratio of 2:1 and was synthesized in-house; 5% stock solutions of SMA were prepared in 1.0 M NaCl and refluxed for 2 h followed by overnight dialysis at 4 °C in 50 mM Tris-HCl (pH 8.0). The composition of the lyophilized product was confirmed by FTIR. ECg was a gift from Mitsui Norin, Tokyo, Japan and was used at a concentration of  $12.5 \text{ mg l}^{-1}$ .

Proteins were separated by sodium dodecyl sulfate-polyacrylamide gel electrophoresis (SDS-PAGE) on a 10% acrylamide/ bis-acrylamide gel matrix and visualized with Coomassie brilliant blue (Sigma-Aldrich) with a limit of detection of 0.2  $\mu\text{g}$ . N-(2-hydroxy-1,1-bis(hydroxymethyl) ethyl) glycine (tricine) modification of SDS-PAGE was also used to avoid aggregation of membrane proteins in the gel, essentially as described by Schagger [10]. Protein-containing samples were concentrated in Vivaspin columns (<10 000 kDa) to approximately  $20 \text{ mg ml}^{-1}$  protein. For Western blotting, proteins were transferred by electrophoresis to Millipore polyvinylidene membranes and probed with antibodies to proteins of interest. Binding was detected with monoclonal secondary antibody conjugated to horseradish peroxidase (HRP) followed by peroxide substrate and Supersignal West Pico Chemiluminescent Substrate (Thermo Scientific), an enhanced chemiluminescence HRP substrate. Different secondary antibodies were used for detection of PBP2 (anti-rabbit) and PBP2a (anti-mouse). For transmission electron microscopy (TEM), suspensions were dropped on a grid, washed twice with 50 mM Tris buffer, stained with uranyl acetate [2] and viewed and photographed using a Philips 201 microscope.

Protein content of nanoparticles was determined by absorbance at 280 nm using a Nanodrop 2000 spectrophotometer. The hydrodynamic particle size distribution of SMALPs was measured by dynamic light scattering (DLS) using a Zetasizer Nano ZS. Samples (1 ml) were placed in a semi-micro PS disposable polystyrene cuvette (Fischer Scientific) and equilibrated at 25 °C for 5 min to ensure temperature homogeneity prior to taking 16 measurements for each sample, repeated three times. Data was analyzed using Zetasizer software (V. 6.20). SMALPs were further characterized with respect to their capacity to induce forward light scatter (FSC; reflecting predominantly size, but also refractive index and shape) and side scatter (SSC; indicative of geometry and internal structure, or 'granularity') using flow cytometry in tandem with fluorescein isothiocyanate (FITC)-coupled second antibodies and excitation at 488 nm, adapted for the analysis of nanoparticles by van der Vlist *et al* [11]. SMALPs (500  $\mu\text{l}$  aliquots) in buffer pH 7.6 were labeled with 60  $\mu\text{M}$  Nile Red (Invitrogen) for 30 min in the dark and detected using a Miltenyi MACSQuant Analyzer with voltage set between 300 V and 500 V, gated for fluorescence (trigger 3.0) and subsequently back gated for SSC and FSC. Twenty thousand events were collected for each sample and data analyzed with Miltenyi MACS Quantify Software. Fluorescence was used as the parameter for setting the acquisition trigger and the trigger level was adjusted to minimize

electronic noise. All assays were performed three times on separate days.

To determine if PBP2 and PBP2a were present in close proximity within nanoparticles and membrane preparations, proteins were cross-linked with 3,3'-Dithiobis (sulfosuccinimidylpropionate) (DTSSP) linked by a spacer arm of 12 Å (Thermo Scientific). DTSSP was dissolved to a final concentration of 10 mM in 300 µl of SMALP solution (25 mg ml<sup>-1</sup> protein) and incubated at 4 °C for 30 min. The cross-linking reaction was quenched by the addition of 2.5 µl of 1 M Tris-HCl, pH 7.5 and incubated for 15 min [12]. Cross-links were cleaved by addition of 5% 2-mercaptoethanol (Sigma) in tricine sample buffer. For immunoaffinity chromatography (IAC), protein G HP spintrap columns (GE Healthcare Life Sciences) were equilibrated in Tris-buffered saline (TBS; 50 mM Tris-HCl, 150 mM NaCl; pH 7.5), antibody bound to the column (0.5–1.0 mg ml<sup>-1</sup> in 200 µl TBS) and excess removed by washing. SMALPs (maximum volume 500 µl) were added to the column, maintained with shaking at 4 °C for 60 min, washed extensively with TBS and centrifuged at 150 g for 1 min at 4 °C. Bound material was eluted from the column with 100 µl 0.1 M glycine pH 2.5 and centrifuged for 1 min at 1000 g; pH was neutralized with 1 M Tris-HCl pH 8.0. For co-immunoprecipitation (Co-IP), paramagnetic beads coated with protein G (Dynal) and complexed with either anti-PBP2 or anti-PBP2a antibodies were used to purify PBP2/PBP2a-containing nanoparticles; SMALPs (200–400 µl protein) were mixed with the Dynabeads and the mixture incubated at 4 °C for 2 h with constant agitation. The complex was eluted following manufacturer's instructions and captured proteins analyzed by SDS-PAGE and Western blotting.

### 3. Results and discussion

Initially, attempts were made to solubilize PBP2/PBP2a complexes from EMRSA-16 membranes with Triton X-100. Cells from 11 cultures were suspended in 1–4 ml of ice-cold distilled water and disrupted using a FastPrep FP120 Homogenizer (Thermo Scientific). Cell wall debris was removed by centrifugation (5000 g; 10 min; 4 °C), CMs collected (130 000 g; 1 h; 4 °C) and the pellet suspended in ~200 µl of 10 mM Tris-HCl (pH 7.0) containing 2% Triton X-100 [8]. Exposure of solubilized proteins to DTSSP followed by Co-IP with anti-PBP2 antibody failed to elicit cross-linked PBP2/PBP2a; only PBP2 could be detected in Western blots of Co-IP eluents separated by SDS-PAGE (figure S1; in the supplementary file, available at [stacks.iop.org/NANO/25/285101/mmedia](http://stacks.iop.org/NANO/25/285101/mmedia)). We also attempted unsuccessfully (data not shown) to cross-link the two proteins after solubilization with 1% formaldehyde (95 °C; 5 min). We conclude that any PBP2/PBP2a complexes are disrupted by detergent extraction; this accords with published reports demonstrating recovery of PBPs by non-ionic detergents in exclusively monomeric form [13, 14]. Consequently, we examined the potential of SMA co-polymer solubilization to reveal the presence of closely associated PBP2/PBP2a.

As the composition of the staphylococcal CM is unusual, we determined if SMA was able to solubilize proteins from purified EMRSA-16 membranes. Cells were suspended in 3 ml 20% sucrose, 0.05 M Tris-HCl, 0.145 M NaCl (pH 7.6) and the cell wall digested with 80 µg lysostaphin (with 25 µg DNase I and protease inhibitors) for 10 min at 37 °C. SMA was added to final concentration of 2.5% and the mixture (6 ml) incubated for 1 h at 37 °C; membranes were collected by centrifugation (100 000 g; 1 h; 4 °C). Proteins were separated by tricine-SDS-PAGE. Western blotting revealed the presence of both PBP2 and PBP2a in SMALPs. As the preparation of bacterial membranes may lead to redistribution of bilayer protein and lipid, we modified this procedure to enable solubilization of PBPs from intact cells; the lysostaphin digestion components were added to 3 ml bacterial suspension from 2 l culture and incubated for 10 min at 37 °C prior to addition of SMA. Omission of this cell wall digestion step resulted in failure to extract membrane proteins; lysostaphin, which disrupts the pentaglycine cross-bridges of peptidoglycan [15], breached the integrity of the cell wall as determined by TEM (figure 1(B)). After addition of SMA and further 50 min incubation, SMALPs were recovered from the supernatant (100 000 g; 1 h; 4 °C). TEM showed that partial digestion of the cell wall was necessary to allow ingress of SMA and egress of SMALPs (figure 1(C)). Initial experiments included sonication of bacteria and 16 h incubation at 37 °C prior to centrifugation, as these steps were considered essential to obtain homogeneous preparations of SMA liposomal extracts [2, 3], but neither were found to be necessary for membrane protein extraction and were omitted from our optimized protocol, as sonication is likely to disrupt physical associations between membrane proteins. The amount of membrane protein extracted from EMRSA-16 by SMA was comparable to that extracted by 2% Triton X-100 (figure S2).

TEM images of material solubilized by SMA from DMPC vesicles, *S. aureus* SH1000 and EMRSA-16 revealed monodispersed, homogeneous suspensions (figure 2) with mean diameters of 12 ± 2 nm (±1SD) for particles from protein-free DMPC vesicles and 18 ± 3 nm and 24 ± 5 nm (all n = 75) for those from SH1000 and EMRSA-16, indicating that incorporation of proteins results in SMALPs of increased size. Nanoparticle size distribution and dispersion were investigated by DLS and flow cytometry (figure 3). DLS confirmed the monodispersed nature of SH1000 and EMRSA-16 preparations and indicated that hydrodynamic diameters of SMALPs were 17.4 ± 2.23 nm and 24.5 ± 2.64 nm, in good agreement with measurements from TEM. Although these nanoparticles are close to the lower limits of detection, they were readily quantified and analyzed by flow cytometry, employing fluorescence threshold triggering to discriminate fluorescently labelled SMALPs from non-fluorescent noise [11]. Figure 3(A) shows the forward- (influenced by size, refractive index, shape) and side-scatter distribution (geometry, internal structure) of nanoparticles from EMRSA-16, visualizing both Nile Red-labeled SMALPs and noise events. SMALPs labeled with the lipophilic dye Nile Red could be discriminated from non-fluorescent noise (figure 3(B)); raising the fluorescence threshold

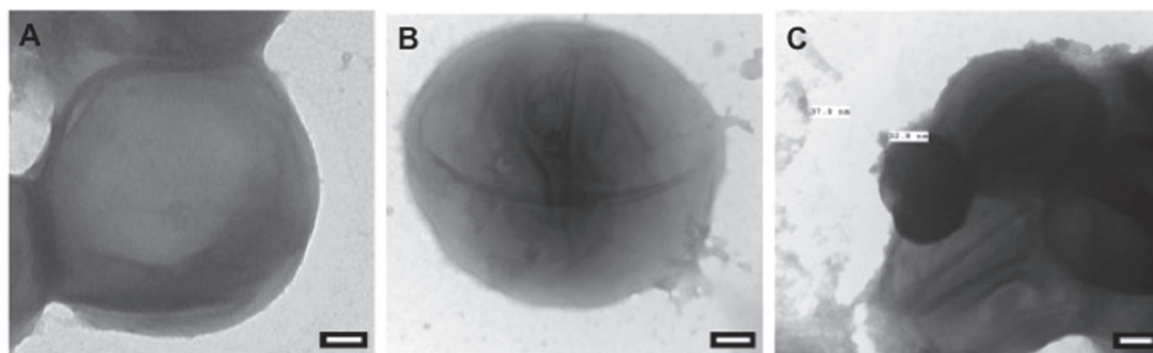


**Figure 1.** TEM of (A) EMRSA-16 cell, (B) after 10 min exposure to lysostaphin ( $26.7 \text{ mg l}^{-1}$ ), (C) after 10 min lysostaphin digestion followed by 2.5% SMA and incubation for 50 min. Two SMALPs of diameter 37.9 nm and 32.8 nm can be seen. Scale bar = 100 nm.

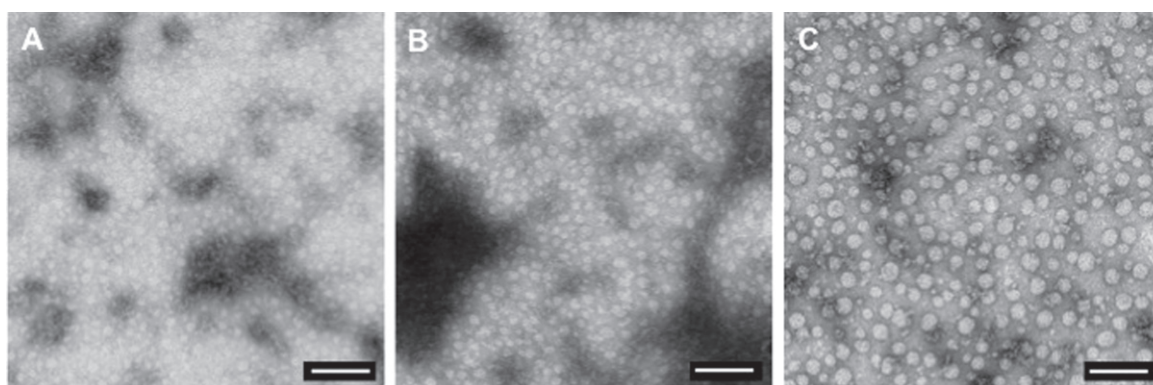


**Figure 2.** TEM of (A) DMPC, (B) SH1000 membranes and (C) EMRSA-16 membranes incorporated into SMALPs. Bacterial membranes were solubilized directly from viable bacteria with no intermediate membrane purification step. Scale bar = 100 nm.

to eliminate noise (figure 3(C)) showed that the majority of particles formed a homogeneous population with respect to forward- and side-scatter but with a short tail of small fluorescent particles (figures 3(C) and (D)). When particles were stained with Nile Red (for lipid) and Bocillin FL (for PBPs) and examined by fluorescence microscopy, the two stains colocalized, indicating successful protein extraction. PBP2 and PBP2a were detected in unfractionated SMALPs from EMRSA-16 by Western blotting.

Protein-containing SMALPs were enriched by IAC or Co-IP; prior to enrichment, proteins separated by 12 Å or less were cross-linked with DTSSP. IAC was employed to determine if PBP2 or PBP2a could be detected in protein complexes recovered using antibodies raised against FtsZ. Western blotting of proteins from EMRSA-16 SMALPs reacting with anti-FtsZ antibodies contained PBP2, PBP2a and FtsZ (figure 4), indicating that these proteins exist on or within the CM in close spatial proximity. IAC and Co-IP with both anti-PBP2 and anti-PBP2a antibodies yielded nanoparticles in which PBP2 and PBP2a, but not FtsZ, could be detected in Western blots with the appropriate antibodies, but the bands were less prominent in comparison to blots of anti-FtsZ-recovered nanoparticles, almost certainly reflecting the low number of copies of PBPs in each *S. aureus* cell [16].

ECg completely abolishes  $\beta$ -lactam resistance in clinical MRSA isolates; it reduces the minimum inhibitory concentration of oxacillin required to prevent growth of EMRSA-

16 from 512 to  $<1 \text{ mg l}^{-1}$ , due to its capacity to intercalate deep within the CM, fundamentally altering the biophysical characteristics of the bilayer and forcing the bacteria to respond by reconfiguration of CM architecture [8, 17]. The polyphenol induces partial delocalization of PBP2 from the septal divisome [8], indicating that reversible sensitization to  $\beta$ -lactam antibiotics may be due to dissipation of the PBP2/PBP2a-facilitated resistance machinery. In this study, it is clear that  $12.5 \text{ mg l}^{-1}$  ECg alters the spatial relationship between these two proteins, as PBP2a can no longer be recovered by SMA extraction and capture with anti-FtsZ antibodies (figure 4), providing support for this supposition.

Eluents from Co-IP were also investigated by analytical flow cytometry. SMALPs were enriched with anti-PBP2 antibodies, lipid labeled with Nile Red and probed with anti-PBP2a antiserum and FITC-conjugated second antibody. Conversely, nanoparticles enriched with anti-PBP2a were probed for the presence of PBP2. In both cases, the partner protein was readily detected, with 8260 of 20 000 reacting with anti-PBP2a antibodies after enrichment with anti-PBP2 antibodies and 7260 of 20 000 with anti-PBP2 antibodies after enrichment with anti-PBP2a antibodies (figure 5). These data provide strong evidence that PBP2 and PBP2a are in close spatial proximity following recruitment by FtsZ and are recovered from the CM in  $\sim 40\%$  of SMALPs. It is likely that this reflects the proportion of PBP2/PBP2a complexes actively involved in cell division, with the remainder

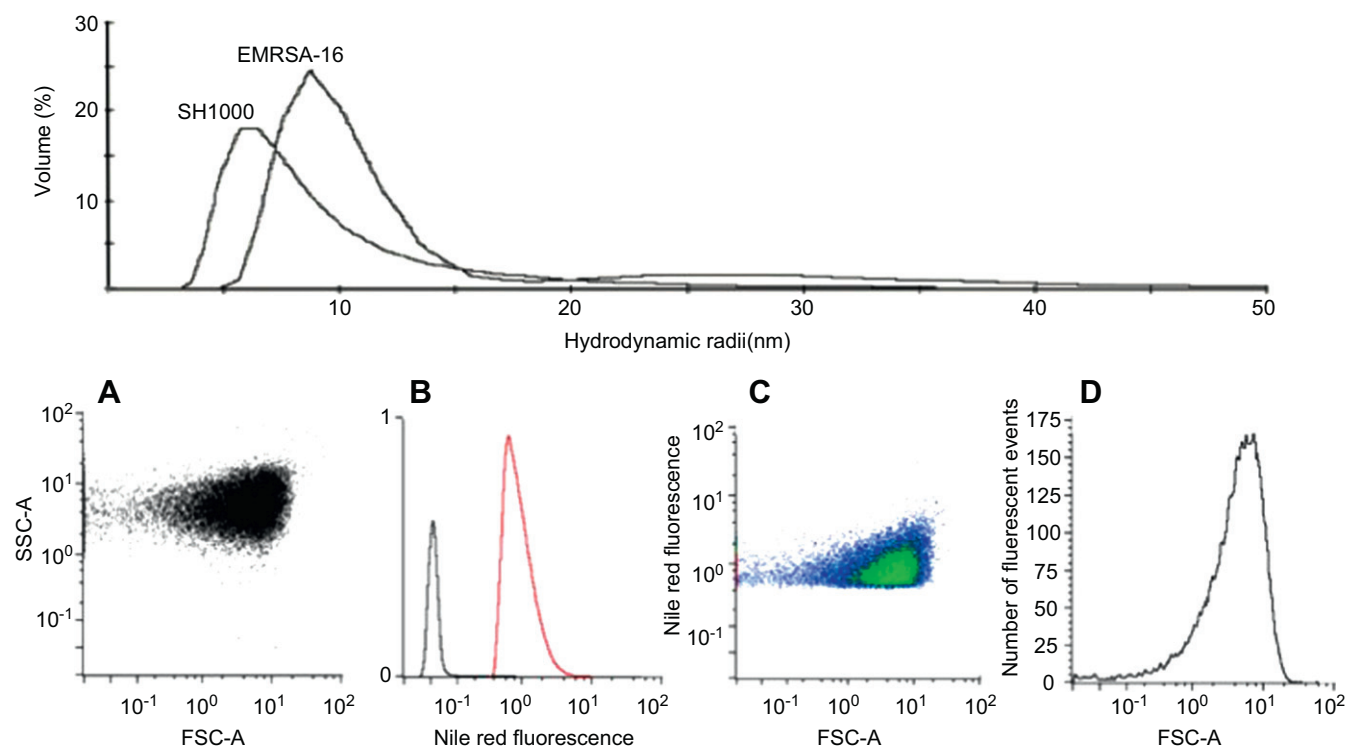


**Figure 3.** Size determination of SMALPs from EMRSA-16 membranes. Upper panel: distribution of hydrodynamic radii determined by DLS. Lower panel: flow cytometry of SMALPs labeled with  $60 \mu\text{M}$  Nile Red by (A) size (forward scatter; FSC-A) and granularity (side scatter; SSC-A), no discrimination between fluorescent and non-fluorescent nanoparticles, all arbitrary units; (B) fluorescence intensity of Nile Red within SMALPs (red) and non-fluorescent SMALPs (black); (C) separation of SMALPs labeled with Nile Red by fluorescence sorting; number of particles in the scatter plot follow the transition from blue (low) through green to red (high); (D) size distribution (FSC-A) of Nile Red-labeled SMALPs.

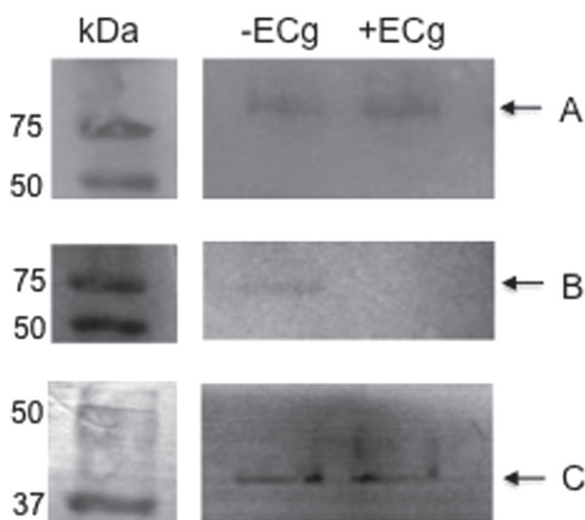


**Figure 4.** Western blots of EMRSA-16 SMALP proteins recovered by anti-FtsZ IAC. Bacteria were grown in the absence (-ECg) or presence (+ECg) of the drug resistance modifier ECg ( $12.5 \text{ mg l}^{-1}$ ) and proteins probed with anti-PBP2 (A), anti-PBP2a (B) and anti-FtsZ (C) antibodies. Arrows indicate the target protein in each blot.

recovered from regions of the membrane other than those accommodating divisome complexes. Flow cytometry provided further evidence that exposure of EMRSA-16 to  $12.5 \text{ mg l}^{-1}$  ECg caused partial dissociation of PBP2/PBP2a

complexes. Co-IP of SMALPs from control and ECg-exposed cells was undertaken with anti-PBP2 and anti-PBP2a antibodies and PBP2 and PBP2a quantified with the appropriate antibody combinations. With anti-PBP2 Co-IP pull down, there was a 1.76-fold reduction in the PBP2/PBP2a ratio following ECg exposure, reflecting a reduction in PBP2a FITC fluorescence (normalized against PBP2 Nile Red fluorescence) from 231.6 arbitrary fluorescence units (AFU) to 131.6 AFU. With anti-PBP2a Co-IP, a 1.43-fold reduction was observed, corresponding to a reduction in normalized PBP2a fluorescence from 53.7 AFU to 37.6 AFU. Flow cytometry scatter plots from these experiments are shown in figure S3. Flow cytometry was used as it is a highly sensitive, quantitative method with a much lower limit of detection compared to semi-quantitative Western blotting. In this context, we were unable to detect a band corresponding to PBP2a by Western blotting of SMA-extracted proteins from ECg-exposed EMRSA-16 cells; flow cytometry clearly indicated residual PBP2a, in agreement with a study showing partial, rather than complete, disruption of the complex [8]. Also of note was our ability to obtain fluorescence data by flow cytometry from nanoparticles of 20–25 nm diameter, using methods [11] designed for detection and analysis of vesicles of  $\sim 100 \text{ nm}$ .

We show for the first time that SMA trapping of membrane domains can be used to extract native membrane-embedded protein complexes directly from intact bacteria.

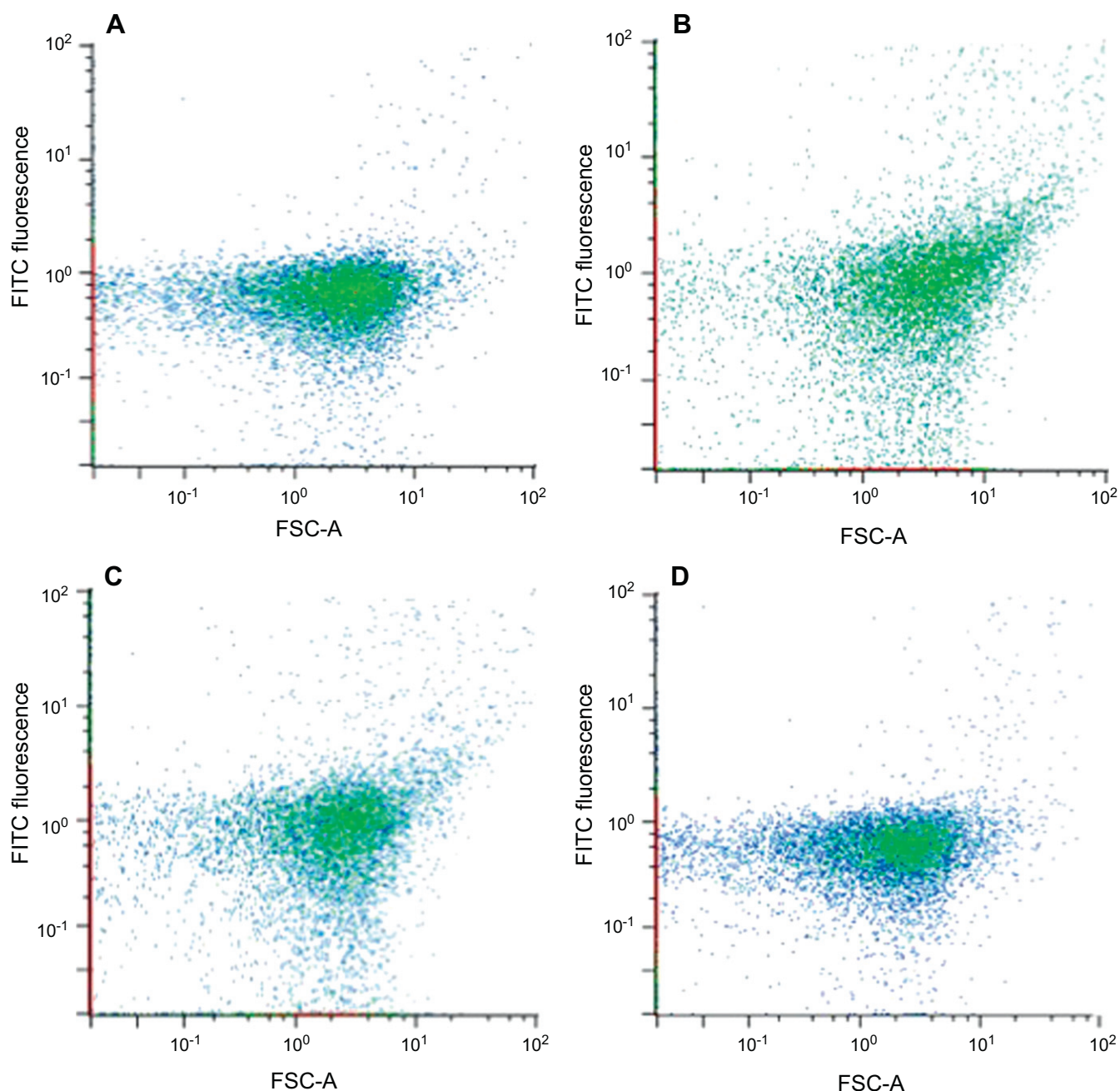


**Figure 5.** Flow cytometry of EMRSA-16 SMALPs enriched for PBP2 and PBP2a by Co-IP. Nanoparticles were labeled with Nile Red and size (forward scatter; FSC-A) and granularity (side scatter; SSC-A) determined after pull down with (A), (B) anti-PBP2 and (C), (D) anti-PBP2a antibodies. Nanoparticles from A were labeled with murine anti-PBP2a antibodies followed by FITC-conjugated anti-mouse IgG secondary antibody (B) and those from B with rabbit anti-PBP2 antibodies and FITC-conjugated anti-rabbit IgG second antibody (D). In each experiment, 20 000 Nile Red-labeled nanoparticles; 8260 reacted with anti-PBP2a antibodies when enriched with anti-PBP2 antibodies (B) and 7260 with anti-PBP2 antibodies when enriched with anti-PBP2 antibodies (D).

Other studies [2–4] have effected removal of single proteins within model lipid bilayers or over-expressed proteins from protoplasts of viable bacteria. The latter approach would not be suitable for SMALP enrichment of divisome proteins as key components remain at the septum due to interactions with D-alanyl-D-alanine termini on nascent peptidoglycan chains [18]; removal of the cell wall will destroy this anchor and delocalize proteins. It was necessary to minimally digest the cell wall whilst retaining overall architecture and we established that 10 min lysostaphin digestion of whole cells led to

optimal cell wall perturbation compatible with protein extraction. SMA solubilized substantial amounts of protein from the membrane but native PBP2 and PBP2a copy numbers are low and this restricted our capacity to purify enough protein using PBP-specific antisera for analysis by Western blotting, but not by the more sensitive flow cytometry technique. In contrast, there are many more copies of FtsZ, the major cytoskeletal protein, within the membrane bilayer [19]. The presence of FtsZ within PBP2/PBP2a-containing nanoparticles could only be demonstrated when anti-FtsZ

antiserum was used for purification by IAC. SMALP capture of FtsZ, PBP2 and PBP2a with antiFtsZ antiserum shows that the procedure can remove large protein complexes. The *S. aureus* division machinery is comprised of many membrane-located and cytosolic proteins that interact with the FtsZ scaffold: removal of functionally active components of the divisome in a spatially relevant manner will provide a new tool for elucidation of their complex interactions.

## Acknowledgements

This work was funded by BBSRC grant BB/1005579/1. SP was supported by a grant from the Royal Pharmaceutical Society of Great Britain, awarded to PWT. The National Institute for Health Research University College London Hospitals Biomedical Research Centre provided further support.

## References

- [1] Egan A J F and Vollmer W 2013 The physiology of bacterial cell division *Ann. New York Acad. Sci.* **1277** 8–28
- [2] Knowles T J, Finka R, Smith C, Lin Y P, Dafforn T and Overduin M 2009 Membrane proteins solubilized intact in lipid containing nanoparticles bounded by styrene maleic acid copolymer *J. Am. Chem. Soc.* **131** 7484–5
- [3] Jamshad M et al 2011 Surfactant-free purification of membrane proteins with intact native membrane environment *Biochem. Soc. Trans.* **39** 813–8
- [4] Orwick-Rydmark M, Lovett J E, Graziadei A, Lindholm L, Hicks M R and Watts A 2012 Detergent-free incorporation of a seven-transmembrane receptor protein into nanosized bilayer lipodisq particles for functional and biophysical studies *Nano Lett.* **12** 4687–92
- [5] Long A R, Malhotra K, Schwall C T, Albert A D, Watts A and Alder N N 2013 A detergent-free strategy for the reconstitution of active enzyme complexes from native biological membranes into nanoscale discs *BMC Biotechnol.* **13** 41
- [6] Johnson A P, Davies A, Guy R, Abernathy J, Sheridan E, Pearson A and Duckworth G 2012 Mandatory surveillance of methicillin-resistant *Staphylococcus aureus* (MRSA) bacteraemia in England: the first 10 years *J. Antimicrob. Chemother.* **67** 802–9
- [7] Fuda C C S, Fisher J F and Mobashery S 2005  $\beta$ -lactam resistance in *Staphylococcus aureus*: the adaptive resistance of a plastic genome *Cell. Mol. Life Sci.* **62** 2617–33
- [8] Bernal P, Lemaire S, Pinho M G, Mobashery S, Hinds J and Taylor P W 2010 Insertion of epicatechin gallate into the cytoplasmic membrane of methicillin-resistant *Staphylococcus aureus* disrupts penicillin-binding protein (PBP) 2a-mediated beta-lactam resistance by delocalizing PBP2 *J. Biol. Chem.* **285** 24055–65
- [9] Adams D W and Errington J 2009 Bacterial cell division: assembly, maintenance and disassembly of the Z ring *Nat. Rev. Microbiol.* **7** 642–53
- [10] Schagger H 2006 Tricine-SDS-PAGE *Nat. Protocols* **1** 16–22
- [11] van der Vlist E J, Nolte-t Hoen E S M, Stoorvogel W, Arkesteijn G J A and Wauben M H M 2012 Fluorescent labeling of nano-sized vesicles released by cells and subsequent quantitative and qualitative analysis by high-resolution flow cytometry *Nat. Protocols* **7** 1311–26
- [12] Bennett K L, Kussmann M, Björk P, Godzwon M, Mikkelsen M, Sørensen P and Roepstorff P 2000 Chemical cross-linking with thiol-cleavable reagents combined with differential mass spectrometric peptide mapping—a novel approach to assess intermolecular protein contacts *Protein Sci.* **9** 1503–18
- [13] Chase H A 1980 Purification of four penicillin-binding proteins from *Bacillus megaterium* *J. Gen. Microbiol.* **117** 211–24
- [14] Di Guilmi A M, Mouz N, Andrieu J P, Hoskins J, Jaskunas S R, Gagnon J, Dideberg O and Vernet T 1998 Identification, purification, and characterization of streptidase and glycosyltransferase domains of *Streptococcus pneumoniae* penicillin-binding protein 1a *J. Bacteriol.* **180** 5652–9
- [15] Schindler C and Schuardt V 1964 Lysostaphin: a new bacteriolytic agent for the staphylococcus *Proc. Natl. Acad. Sci. USA* **51** 414–21
- [16] Pucci M J and Dougherty T J 2002 Direct quantitation of the numbers of individual penicillin-binding proteins per cell in *Staphylococcus aureus* *J. Bacteriol.* **184** 588–91
- [17] Palacios L, Rosado H, Micol V, Rosato A, Bernal P, Arroyo R, Grounds H, Anderson J C, Stabler R A and Taylor P W 2014 Staphylococcal phenotypes induced by naturally occurring and synthetic membrane-interactive polyphenolic  $\beta$ -lactam resistance modifiers *PLoS One* **9** e93830
- [18] Pinho M G and Errington J 2003 Dispersed mode of *Staphylococcus aureus* cell wall synthesis in the absence of the division machinery *Mol. Microbiol.* **50** 871–81
- [19] Erickson H P, Anderson D E and Osawa M 2010 FtsZ in bacterial cytokinesis: cytoskeleton and force generator all in one *Microbiol. Mol. Biol. Rev.* **74** 504–28